Chemical Science

EDGE ARTICLE

View Article Online
View Journal | View Issue

Cite this: *Chem. Sci.*, 2014, **5**, 2072

Photoinduced electron transfer in a carbon nanohorn–C_{60} conjugate†

María Vizuete,[a] Maria José Gómez-Escalonilla,[a] José Luis G. Fierro,[b] Kei Ohkubo,[c] Shunichi Fukuzumi,*[cd] Masako Yudasaka,[e] Sumio Iijima,[f] Jean-François Nierengarten[g] and Fernando Langa*[a]

Received 5th December 2013
Accepted 6th February 2014

DOI: 10.1039/c3sc53342e

www.rsc.org/chemicalscience

A nanohybrid combining two allotropic forms of carbon, namely carbon nanohorns (CNH) and C_{60}, has been obtained from a C_{60} derivative bearing a benzocrown ether subunit (crown–C_{60}) and a CNH functionalized with NH_3^+ groups (CNH-sp-$NH_3^+F^-$) through ammonium–crown ether interactions. The resulting CNH–C_{60} nanohybrid has been characterized by Raman and XPS spectroscopies, thermogravimetric analysis (TGA) and high-resolution transmission electron microscopy (HR-TEM). The photophysical properties of the CNH–C_{60} conjugate have been investigated in benzonitrile. Femtosecond laser flash photolysis measurements revealed the occurrence of an efficient electron transfer from the singlet excited state of the C_{60} moiety to the CNH with a rate constant of 6.5×10^{10} s^{-1} to produce a radical ion pair, which decayed by charge recombination with a lifetime of 1.0 ns to afford the triplet excited state of CNH-sp-$NH_3^+F^-$ and crown–C_{60}. The two carbon nanoforms play therefore complementary roles in the CNH–C_{60} conjugate, the CNH acting as an electron donor and C_{60} as an electron acceptor.

Introduction

Since the discovery of carbon nanotubes (CNTs) by Iijima,[1] these fascinating materials have attracted enormous attention at both academic and technological levels.[2–9] Among the wide range of carbon nanomaterials, carbon nanohorns (CNHs)[10,11] consisting of pseudo-cylindrical single-wall tubules with a conical tip are closely related to CNTs. The diameter of the tubular part of CNHs is *ca.* 2–4 nm with lengths of 30 to 50 nm, and they typically form radial aggregates (*dahlia-like*) of *ca.* 80 nm in diameter. One advantage of CNHs is related to their metal-free synthesis. Indeed, they are generally produced in high yields by laser ablation of pure graphite. As such, CNHs thus obtained are essentially metal-free and very pure (around 95%). Moreover, acidic treatments to remove the metal particles are not necessary as in the case of single-wall carbon nanotubes (SWCNTs). Partial degradation of the graphitic structures by strong acids is thus avoided. Therefore, pure samples of CNHs are available more easily than pure samples of SWCNTs, which favours their applications.[12,13]

Carbon-based nanostructured materials such as fullerenes, graphenes and CNTs constitute a unique platform for energy conversion systems, for example, for photovoltaics and opto-electronics. Although the preparation of hybrid structures combining CNTs with electron donor moieties has been widely reported,[14–18] the combination of CNTs with electron acceptors in which the carbon nanoform is acting as an electron donor is unusual and remains fairly unexplored.[19,20] Among all of the electron acceptor systems, hybrids between SWCNTs and fullerenes have attracted a great deal of attention in the past few years owing to their outstanding optical and electronic properties.[21–23]

Such photoactive materials are attractive candidates to produce electrical energy when irradiated.[21] However, a drawback of SWCNTs for electronic applications is related to the fact that they are obtained as mixtures of compounds having different conducting properties, *i.e.* metallic or semiconducting.[14] Indeed only the latter ones are of interest for the construction of nano-scale semiconductor devices.[15] In contrast, *pristine* CNHs show only semiconducting properties[16] making them, together to their higher purity and homogeneity aspects (*vide supra*), of great interest for nanotechnological applications.[9c]

[a]*Instituto de Nanociencia, Nanotecnología y Materiales Moleculares (INAMOL), Universidad de Castilla-La Mancha, 45071, Toledo, Spain. E-mail: Fernando.Langa@uclm.es*

[b]*Instituto de Catálisis y Petroleoquímica, Cantoblanco, 28049, Madrid, Spain*

[c]*Department of Material and Life Science, Graduate School of Engineering, Osaka University, ALCA, Japan Science and Technology Agency (JST), Suita, Osaka 565-0871, Japan. E-mail: fukuzumi@chem.eng.osaka-u.ac.jp*

[d]*Department of Bioinspired Science, Ewha Womans University, Seoul 120-750, Korea*

[e]*Nanotube Research Center, National Institute of Advanced Industrial and Technology, Higashi, Tsukuba, Ibaraki 305-8565, Japan*

[f]*Department of Physics, Meijo University, Shiogamaguchi, Tenpaku-ku, Nagoya 468-8502, Japan*

[g]*Laboratoire de Chimie des Matériaux Moléculaires, Université de Strasbourg et CNRS, Ecole Européenne de Chimie, Polymères et Matériaux, 25 rue Becquerel, 67087 Strasbourg Cedex 2, France*

† Electronic supplementary information (ESI) available: Spectral, transient absorption and XPS data (Fig. S1–S7 and Tables S1 and S2). See DOI: 10.1039/c3sc53342e

Despite the fact that CNHs show interesting properties for optoelectronics, their photophysical behaviour in donor–CNH nanohybrids has been scarcely considered. Actually, the behaviour of CNHs when doped with electron acceptors, although important, is still unknown. As part of this research, we now report the synthesis and photophysical properties of a CNH–C_{60} nanoensemble (Scheme 1). The nanohybrid has been obtained from a C_{60} derivative bearing a benzocrown ether subunit (crown–C_{60}) and a CNH functionalized with NH_3^+ groups (CNH-sp-$NH_3^+F^-$) through ammonium–crown ether interactions. Importantly, the photophysical investigations of the resulting CNH–C_{60} conjugate have revealed that the two carbon nanoforms play complementary roles, the CNH acting as electron donor and C_{60} as an electron acceptor.

Results and discussion

1 Preparation of the CNH–C_{60} nanohybrid

The formation of the CNH–C_{60} hybrid was achieved from CNH-sp-$NH_3^+F^-$. This derivative was prepared *in situ* by quantitative deprotection of CNH-sp-NH-Boc (Boc = *tert*-butoxycarbonyl) with tetra-*n*-butylammonium fluoride (TBAF) at 0 °C in dichloromethane (see Experimental section, Scheme 3).[23d] The cleavage of the Boc protecting group was clearly confirmed by photoelectron spectroscopy (see ESI, Fig. S1†). CNH-sp-$NH_3^+F^-$ and the benzo-18-crown-6-ether functionalized pyrrolidinofullerene (crown–C_{60})[24] were sonicated in *N*-methylpyrrolidone (NMP) and stirred overnight at room temperature. After removal of the solvent, washing with dichloromethane (to remove the excess of crown–C_{60}) and drying under vacuum, the CNH–C_{60} hybrid was obtained as a black solid. Owing to the presence of long alkyl chains, the hybrid was soluble in dichloromethane (CH_2Cl_2), dimethylformamide (DMF) and benzonitrile (PhCN). The resulting nanohybrid CNH–C_{60} was characterized by a number of analytical techniques, including thermogravimetric analysis (TGA), XPS spectroscopy, high-resolution transmission electron microscopy (HR-TEM), Raman, as well as steady-state and time-resolved spectroscopic techniques.

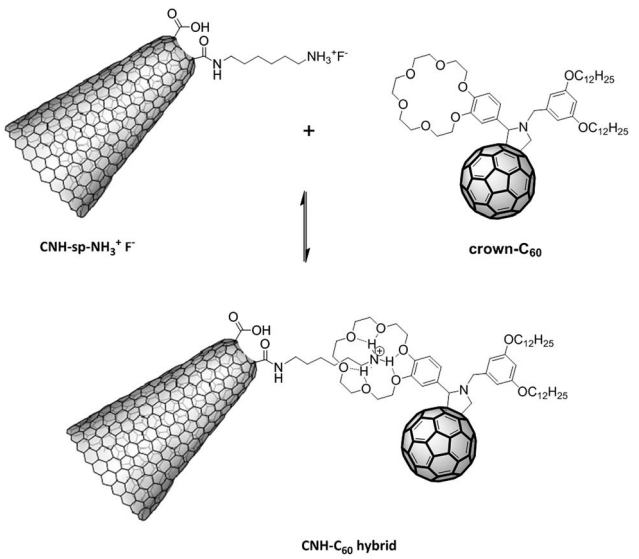

Scheme 1 Formation of CNH–C_{60} hybrid.

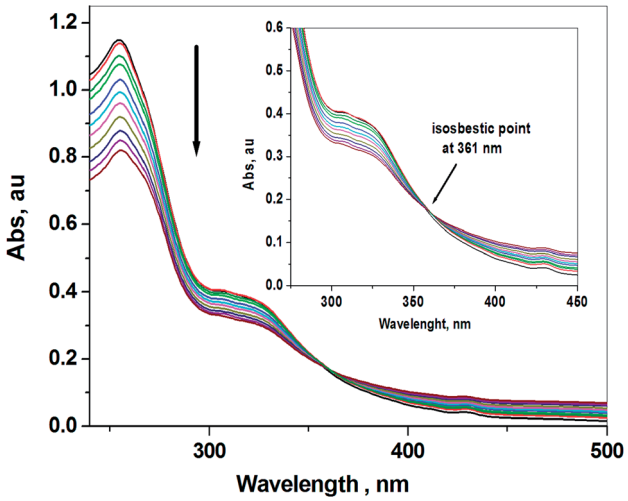

Fig. 1 Absorption spectral changes in the UV-vis spectrum of crown–C_{60} (black line: 7.15×10^{-6} M in CH_2Cl_2) on addition of increasing amounts of CNH-sp-NH_3^+ (concentration 1 mg per 100 mL; from 200 μL to 1800 μL, in 2 mL CH_2Cl_2); (inset) spectra of wavelength expansion, showing an isosbestic point at $\lambda = 361$ nm.

The successful functionalization of CNH-sp-$NH_3^+F^-$ with crown–C_{60} was first evidenced by UV-vis spectroscopic titrations in CH_2Cl_2 and PhCN. The changes in the UV-vis spectra of a CH_2Cl_2 solution of crown–C_{60} upon addition of CNH-sp-NH_3^+ are shown in Fig. 1. The intensity of the absorption band at $\lambda = 255$ nm (assigned to the crown–C_{60}) decreases on addition of CNH-sp-NH_3^+. Additionally, the presence of an isosbestic point at $\lambda = 361$ nm clearly indicates the formation of the CNH-sp-NH_3^+/crown–C_{60} nanohybrid (see Fig. 1, inset). Similar results were obtained when the titration was performed in PhCN solution (see Fig. S2, ESI†). A similar trend has been previously observed by D'Souza *et al.* during titrations of fullerene ammonium derivatives with crown ethers, where

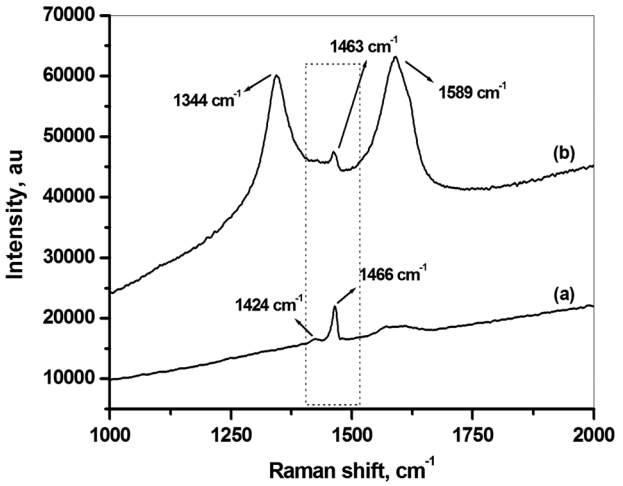

Fig. 2 Raman spectra of crown–C_{60} (a) and CNH-sp-NH_3^+/crown–C_{60} nanohybrid (b) excited at 532 nm.

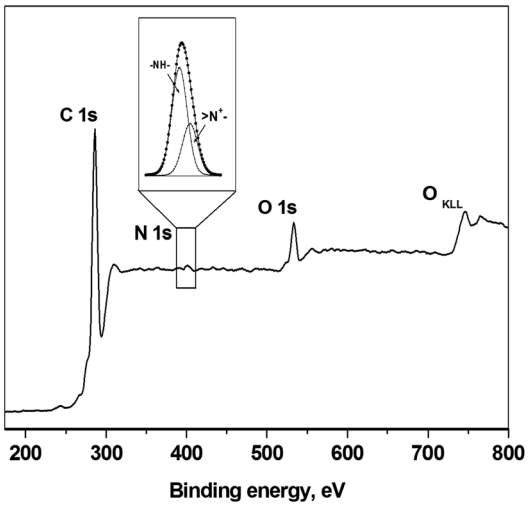

Fig. 3 XPS survey spectra of CNH-sp-NH_3^+/crown–C_{60} nanohybrid.

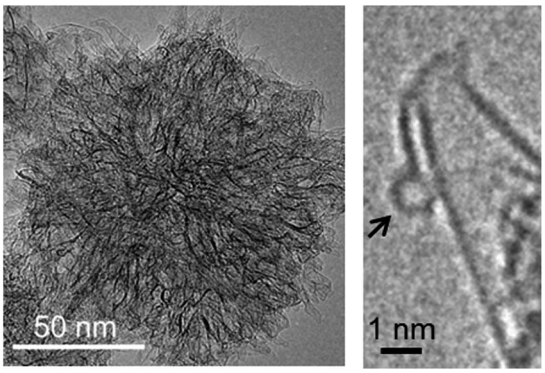

Fig. 4 HR-TEM images of CNH–C_{60} nanohybrid. Aggregates kept the spherical shapes (left panel) and the C_{60} moieties showed spherical shapes (arrow in right panel).

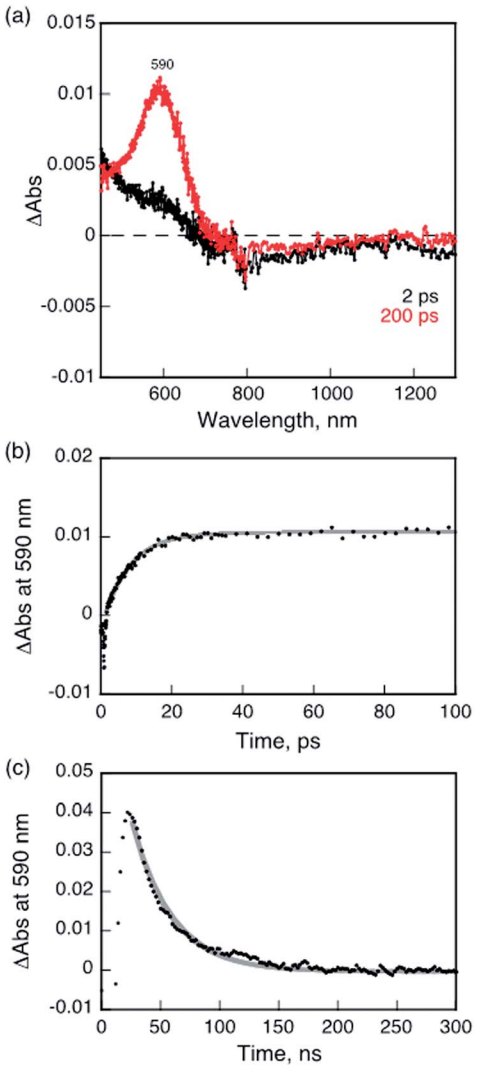

Fig. 5 (a) Transient absorption spectra observed upon femtosecond laser excitation at 393 nm of a PhCN solution of CNH-sp-NH_3^+ (0.5 mg mL^{-1}). (b) Time profile of absorbance at 590 nm in the 0–100 ps time range. (c) Time profile of absorbance at 590 nm in the 0–300 ns time range.

binding constants of 10^3 M^{-1} were obtained.[25] Unfortunately, we were not able to deduce the binding constant as the molecular weight of the CNHs is unknown. Finally, a control experiment was also performed by adding increasing amounts of pristine CNH to a solution of crown–C_{60} (see Fig. S3, ESI†), with no observation of isosbestic points. These results clearly further support the formation of the nano-emsembled through ammonium–crown-ether interactions.

The thermogravimetric analysis (TGA) showed a loss of weight of about 4% for CNH–COOH, 16.5% for CNH-sp-NH_3^+ and 41% for [CNH-sp-NH_3^+/crown–C_{60}] at 500 °C (Fig. S4 in ESI†). The corrected weight losses for CNH-sp-NH_3^+ and CNH-sp-NH_3^+/crown–C_{60} *vs.* CNH–COOH correspond to the losses of the functional groups on the modified CNHs and were estimated to be 12% and 37%, respectively. The number of functional groups in CNH-sp-NH_3^+ was thus estimated as 1 per 100 carbon atoms. With the same calculation, we estimated the amount of functional groups as 1 per 238 carbon atoms for CNH-sp-NH_3^+/crown–C_{60}. This number is however not significant because the thermogram of crown–C_{60} also reveals a 44% loss of weight at 500 °C. Considering that the difference in weight losses observed for CNH-sp-NH_3^+ and CNH-sp-NH_3^+/crown–C_{60} (*ca.* 25%) corresponds to the crown–C_{60} moiety, the amount of crown–C_{60} moiety in CNH-sp-NH_3^+/crown–C_{60} may correspond to a real ratio of *ca.* 56%. Then, the number of functional groups can be estimated as one crown–C_{60} subunit per 110 carbon atoms. Considering the error range of TGA measurements, we can thus estimate a similar functionalization degree for CNH-sp-NH_3^+ and CNH-sp-NH_3^+/crown–C_{60}.

Additional information about the structural and electronic features of CNH–C_{60} was derived from Raman experiments. The spectrum of the crown–C_{60} (Fig. 2) shows the $A_g(2)$ mode at 1466 cm^{-1}, and an additional H_g mode is seen at 1424 cm^{-1}.[26] The CNH-sp-NH_3^+/crown–C_{60} nanohybrid (Fig. 2) shows three peaks at 1589, 1344 and 1463 cm^{-1}. The peaks at 1589 and 1344 cm^{-1} are associated to the G (tangential-mode) and D (disorder-mode) bands of the CNHs surface and the observed peak at 1463 cm^{-1} is assigned to the $A_g(2)$ mode of the C_{60} cage,

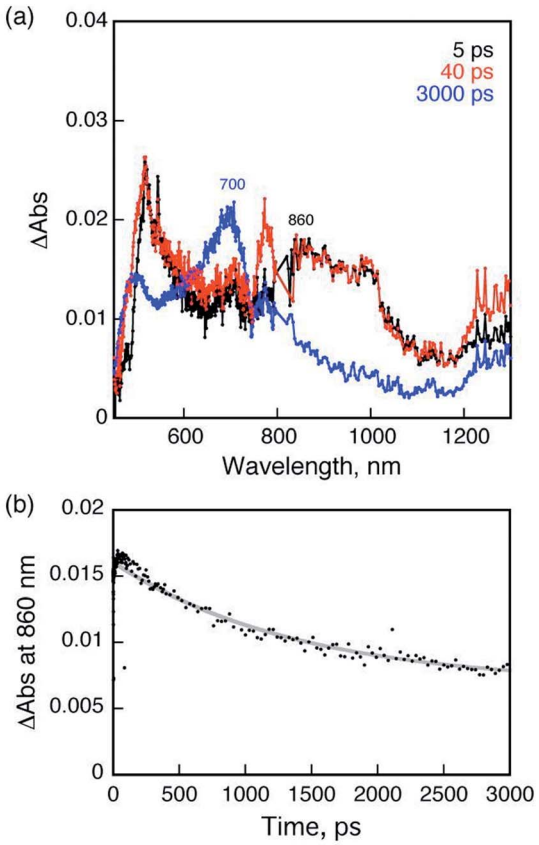

Fig. 6 (a) Transient absorption spectra observed upon femtosecond laser excitation at 393 nm of a PhCN solution of crown–C_{60} (2.0×10^{-4} M). (b) Time profile of absorbance at 860 nm.

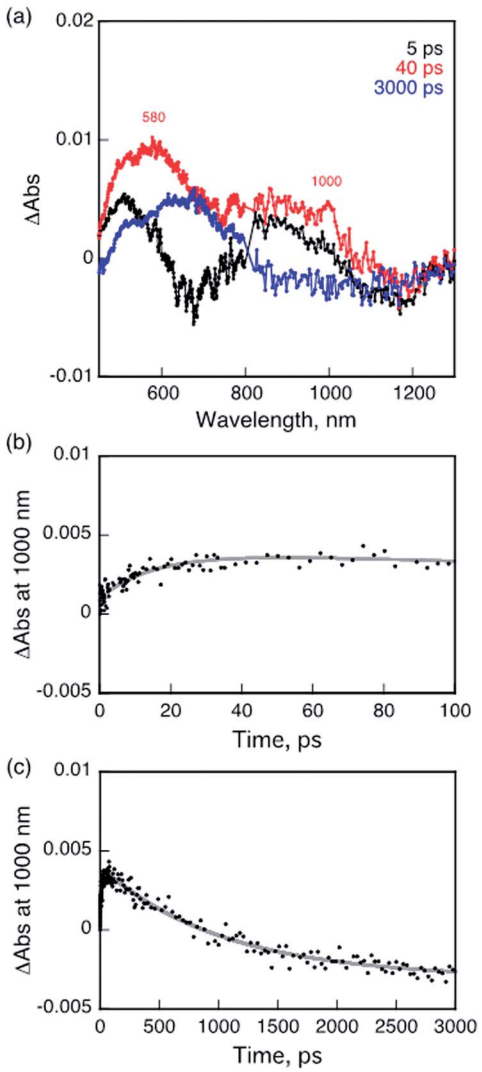

Fig. 7 (a) Transient absorption spectra observed upon femtosecond laser excitation at 393 nm of a PhCN solution of CNH-sp-NH_3^+ (0.5 mg mL^{-1}) and crown–C_{60} (2.0×10^{-4} M). (b) Time profile of absorbance at 1000 nm up to 100 ps. (c) Time profile of absorbance at 1000 nm up to 3000 ns. Time profile at 860 nm is shown in ESI Fig. S7.†

confirming the incorporation of the crown–C_{60} moiety onto CNH-sp-NH_3^+/crown–C_{60} nanohybrid.

Further insight on the formation of the CNH-sp-NH_3^+/crown–C_{60} nanohybrid was revealed by photoelectron spectroscopy (XPS). Its survey spectrum (see Fig. 3) showed only C 1s, O 1s and N 1s emissions but no fluorine was detected.

As shown in Fig. S5 and Table S1 in ESI,† the C 1s line was curve-resolved with only three components: a major one at 284.8 eV (C–C bonds), another at 285.3 eV (sp^3 C), and third one at 286.3 eV (C–O). Consistent with CNH-sp-NH_3^+, the nanohybrid showed two O 1s components at 531.9 and 533.1 eV, which appear slightly shifted to lower BEs values than that found in the former. A similar shift was also observed in the N 1s components (399.0 and 400.0 eV).

The nanohybrid presents three different nitrogen environments (see Scheme 1). The N 1s profile is curve-resolved with only two components at 399.0 and 400.0 eV (the intensity of the former is almost twice that of the later) even though the nanohybrid contains three different nitrogen environments (see Scheme 1). Thus, these observations can be interpreted in terms of the coordination of NH_3^+ group (400.0 eV) to the crown–C_{60}. It was also observed that the oxygen content (to some extent nitrogen) of the nanohybrid [CNH-sp-NH_3^+/crown–C_{60}] is lower than that recorded for CNH-sp-NH_3^+ (Table S2†). Although a dilution effect of the C_{60} moiety is expected, partial coverage of O-atoms from the CNH substrate by C_{60} might well be responsible for that decrease.

The CNH–C_{60} nanohybrid was observed with high-resolution transmission electron microscopy (HR-TEM). The images showed that the CNHs aggregate kept the spherical forms, and the C_{60} moieties were observed in the hybrids (Fig. 4).

2 Photodynamics of CNH–C_{60} nanohybrid

Upon femtosecond laser excitation of a PhCN solution of CNH-sp-NH_3^+, a new transient absorption band appeared at 590 nm at 200 ps as shown in Fig. 5a. The UV-vis-NIR spectrum of CNH-sp-NH_3^+ exhibited no distinct absorption maxima, but only flat absorption in whole region from the IR to the UV region (see ESI Fig. S6†). For transient absorption measurements, we excited CNH at 393 nm, which is in the high energy region. The distinct absorption of the triplet CNH at 590 nm as

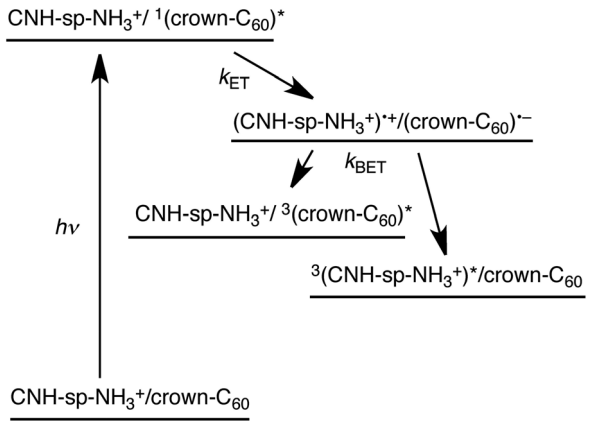

Scheme 2 Reaction course of photoinduced chemical event of the CNH-sp-NH_3^+/crown–C_{60} nanohybrid. It should be noted that each energy level may be changed depending on the radius of CNH-sp-NH_3^+.

shown in Fig. 5a suggest that the fast relaxation may occur from higher excited states to the lowest excited state at the curved edge moiety of CNH. The rate of rise in absorbance at 590 nm obeyed first-order kinetics and the first-order rate constant was determined to be 1.3×10^{11} s^{-1}. This rate constant is similar to that reported for the intersystem crossing from the singlet-excited state (S1) of single-wall carbon nanotubes to the triplet excited state (T1), 5.0×10^{10} s^{-1}.[27,28] No significant decay of the absorbance at 590 nm was observed at the time range of our femtosecond laser flash photolysis (*ca.* 3 ns). The decay process of the triplet-excited state of CNH-sp-NH_3^+ was monitored by nanosecond time-resolved transient absorption spectroscopy (pulse width: 8 ns). A similar transient absorption ($\lambda_{max} = 590$ nm) was observed at 30 ns after laser excitation at 355 nm. The lifetime was determined to be 34 ns in deaerated PhCN (Fig. 5c). Further insight into the nature of this long-lived excited state can be obtained from experiments that probe CNH-sp-NH_3^+ excited-state dynamics in O_2-saturated PhCN. The lifetime of the triplet excited state in O_2-saturated PhCN (30 ns) is slightly shorter than that in deaerated PhCN. This CNH-sp-NH_3^+ excited state exhibits triplet dioxygen quenching dynamics reminiscent of those of triplet excited states of fullerenes.[29] Thus, the absorption band at 590 nm can be assigned to the triplet excited state of CNH-sp-NH_3^+.

Fig. 6a shows transient absorption spectra of crown–C_{60} obtained by femtosecond laser excitation at 393 nm in PhCN. The transient absorption band at 860 nm that appeared at 5 ps decayed at 3000 ps, accompanied by appearance of a new absorption band at 700 nm. These bands at 860 and 700 nm are diagnostic of those due to the singlet and triplet excited states of pyrrolidinofullerenes, respectively.[30] The rate constant of the intersystem crossing was determined from the decay time profile of absorbance at 860 nm (Fig. 6b) to be 7.2×10^8 s^{-1}, which is similar to the value reported for fullerenes.[31,32]

Femtosecond laser excitation at 393 nm of a PhCN solution of CNH-sp-NH_3^+/crown–C_{60} nanohybrid afforded quite different transient spectra from those of each component as shown in Fig. 7a. The initial transient absorption spectrum observed at 5 ps after femtosecond laser excitation exhibits an absorption band at 860 nm, which is the same as that of the singlet excited state of crown–C_{60}, but this is changed to new transient absorption at 580 nm and 1000 nm at 40 ps (Fig. 7a). The absorption band at 1000 nm agrees with that due to pyrrolidinofullerene radical anion.[30,33] This indicates that electron transfer from CNH-sp-NH_3^+ to the singlet excited state of crown–C_{60} occurred to produce the radical cation of CNH-sp-NH_3^+ and the radical anion of crown–C_{60} in the nanohybrid. Thus, the transient absorption band at 580 nm is assigned to the radical cation of CNH-sp-NH_3^+.

The rate constant of electron transfer from CNH-sp-NH_3^+ to the singlet excited state of crown–C_{60} was determined from the rise in absorbance at 1000 nm to be 6.5×10^{10} s^{-1}. The transient absorbance band at 1000 nm due to the radical anion of crown–C_{60} disappeared at 3000 ps, accompanied by appearance of broad absorption at 600–700 nm, which is most likely a superposition of the absorption band at 590 nm due to the triplet excited sate of CNH-sp-NH_3^+ and the absorption band at 700 nm (Fig. 5a) due to the triplet excited state of crown–C_{60} (Fig. 6a). Thus, back electron transfer from the radical anion of crown–C_{60} to the radical cation of CNH-sp-NH_3^+ is proposed to occur, producing the triplet excited states of CNH-sp-NH_3^+ and crown–C_{60}. Because the energy of triplet excited state of CNH-sp-NH_3^+ may be lower than that of crown–C_{60} as reported for carbon nanotubes,[34] the triplet excited state of CNH-sp-NH_3^+ may be the main product of the back electron transfer in the charge-separated state. The rate constant of the back electron transfer was determined from the decay of absorbance at

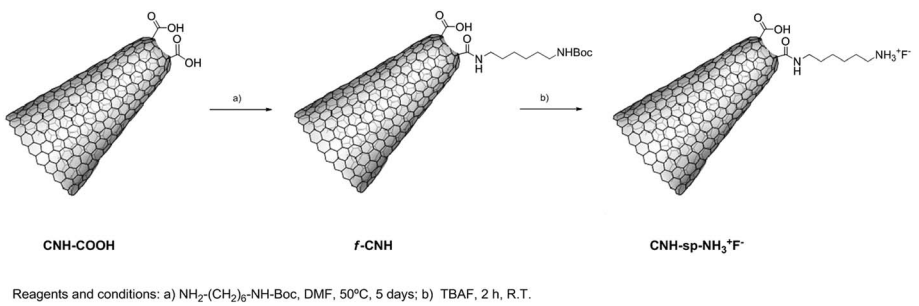

Scheme 3 Synthetic route towards CNH-sp-$NH_3^+F^-$.

1000 nm to be 9.7×10^8 s^{-1} (Fig. 7c), which corresponds to the lifetime of the charge-separated state (1.0 ns). The reaction course of photoinduced chemical event of the CNH-sp-NH_3^+/crown–C_{60} nanohybrid is summarized in Scheme 2.

Conclusions

CNHs substituted with NH_3^+ moieties (CNH-sp-$NH_3^+F^-$) have combined to a C_{60} derivative bearing a crown ether subunit (crown–C_{60}) to generate a CNH–C_{60} nanohybrid. The amount of functional groups has been estimated as 1 per 110 carbon atoms for the CNH-sp-NH_3^+/crown–C_{60} nanohybrid by TGA measurements. Femtosecond laser excitation of the crown–C_{60} moiety resulted in formation of the singlet excited state [^{1}(crown–C_{60})*], followed by efficient electron transfer from the CNH-sp-NH_3^+ moiety to ^{1}(crown–C_{60}).* The charge-separated state [(CNH-sp-NH_3^+)$^{\bullet+}$/(crown–$C_{60}^{\bullet-}$)] thus generated decays by back electron transfer to afford either the triplet excited states of CNH-sp-NH_3^+ or crown–C_{60}. This is the first example in which the CNHs act as an electron donor, thus opening new perspectives of the design of all-carbon nanomaterials for solar energy conversion.

Experimental section

Materials

Benzonitrile (PhCN) was dried according to published procedures[35] and distilled under argon prior to use. Commercially available chemicals were used without further purification unless otherwise indicated. CNHs were produced by CO_2 laser ablation of graphite in the absence of any metal catalyst under an argon atmosphere (760 Torr) at room temperature; the purity of CNHs was as high as >90% with less amorphous carbons. Then, CNHs was treated with an H_2O_2 aqueous solution at about 100 °C generating the corresponding carboxylic acid groups in CNH–COOH.[36]

Synthesis of crown–C_{60}.[24] This compound was prepared by following a previously reported procedure.

Synthesis of CNH-sp-$NH_3^+F^-$. CNH–COOH (50 mg) was suspended in 100 mL of DMF and the resulting mixture was sonicated for 5 min. *N*-Boc-1,6-diaminohexane (Boc = *tert*-butoxycarbonyl, 150 mg, 0.6 mmol) was then added and the resulting mixture stirred at 50 °C during 5 days to obtain f-CNH (see Scheme 3), which was recovered by vacuum filtration over Millipore employing 0.1 μm fluorophore membrane. The resulting compound was extensively washed with DMF, CH_2Cl_2 and Et_2O and dried under high vacuum. To produce CNH-sp-$NH_3^+F^-$, the Boc protecting group was cleaved by adding a 1 M tetra-*n*-butylammonium fluoride (TBAF) solution in THF (10 mL) to a suspension of f-CNH in CH_2Cl_2 (40 mL) cooled by an ice-water bath under Argon. After 2 h, the reaction mixture was filtered on a Millipore membrane (PTFE, 0.1 μm). The solid was suspended in CH_2Cl_2 with sonication and filtered through a 0.1 μm PTFE membrane. The solid material was washed with EtOH and finally dried under high vacuum to afford 54 mg of CNH-sp-$NH_3^+F^-$.

Synthesis of [CNH-sp-NH_3^+; crown–C_{60}]. CNH-sp-$NH_3^+F^-$ (6.5 mg) was dissolved in *N*-methylpyrrolidone (10 mL) and 10^{-3} M solution of crown–C_{60} in *N*-methylpyrrolidone was added. The reaction mixture was sonicated for 5 min and stirred overnight at room temperature. The hybrid material, namely [CNH-sp-NH_3^+; crown–C_{60}], was obtained as a black solid by filtration of the reaction mixture through 0.1 mm PTFE filter. The filtrate was washed with dichloromethane (4 × 20 mL) to remove the excess of crown–C_{60} and dried under vacuum affording 2.8 mg of the nanohybrid.

Raman spectroscopy. Raman spectra were collected at room temperature using a Renishaw in Via Raman microscope equipped with a CCD camera and a Leica microscope. As an excitation source a Nd:TAG 532 nm was used. Measurements were taken with 10 s exposure times varying the number of accumulations. The laser spot was focused on the sample surface using a long working distance 50× objective. Raman spectra were collected on numerous spots on the sample and recorded with Peltier cooled CCD camera. All spectra were recorded on solid samples over several regions and were referenced to the silicon line at 520 cm^{-1}. The data was collected and analysed with Renishaw Wire and Origin software.

XPS. X-Ray photoelectron spectra (XPS) were obtained with a VG Escalab 200R spectrometer equipped with a hemispherical electron analyser and a Mg-Kα ($h\nu = 1254.6$ eV, 1 eV = 1.6302×10^{-19} J) X-ray source, powered at 120 W. Survey and high resolution spectra were recorded at pass energy of the analyser of 200 and 20 eV, respectively. Binding energies were calibrated relative to the C 1s peak at 284.8 eV. High-resolution spectra envelopes were obtained by curve fitting synthetic peak components using the software "XPS peak". Atomic ratios were computed from experimental intensity ratios and normalized by atomic sensitivity factors.

TGA. The thermogravimetric analysis was performed using a TGA/DSC Linea Excellent instrument by Mettler-Toledo, collected under an inert atmosphere of nitrogen, with a rate of 10 °C min^{-1}, and the weight changes were recorded as a function of temperature.

HR-TEM. For the microscopy, the CH_2Cl_2 dispersion of the complex specimens were dropped on carbon coated copper grids placed on the filtration papers. To remove the uncomplexed fullerene–crown complex we further added a droplet of CH_2Cl_2 several times and dried in nitrogen gas flow atmosphere. The specimens were observed with transmission electron microscopy (TOPCON 002B, Toncon Corporation) at an acceleration voltage of 120 kV. The images were captured and analyzed with CCD system (Ultrascan 1000, GATAN).

UV-vis absorption spectral measurements. Steady-state absorption spectra in the visible and near-IR regions were measured on a Shimadzu UV 3600 spectrometer.

Femtosecond laser flash photolysis measurements. Measurements of transient absorption spectra of CNH-sp-NH_3^+/crown–C_{60} nanohybrid were performed according to the following procedures. An N_2-saturated PhCN solution of dispersed CNH-sp-NH_3^+/crown–C_{60} nanohybrid was excited using an ultrafast source, Integra-C (Quantronix Corp.), an

optical parametric amplifier, TOPAS (Light Conversion Ltd.), and a commercially available optical detection system, Helios provided by Ultrafast Systems LLC. The source for the pump and probe pulses were derived from the fundamental output of Integra-C (λ = 786 nm, 2 μJ per pulse and fwhm = 130 fs) at a repetition rate of 1 kHz. 75% of the fundamental output of the laser was introduced into a second harmonic generation (SHG) unit: Apollo (Ultrafast Systems) for excitation light generation at λ = 393 nm, while the rest of the output was used for white light generation. The laser pulse was focused on a sapphire plate of 3 mm thickness and then white light continuum covering the visible region from λ = 410 nm to 800 nm was generated *via* self-phase modulation. A variable neutral density filter, an optical aperture, and a pair of polarizer were inserted in the path in order to generate a stable white light continuum. Prior to generating the probe continuum, the laser pulse was fed to a delay line that provides an experimental time window of 3.2 ns with a maximum step resolution of 7 fs. In our experiments, the light of SHG output at λ = 393 nm was focused at the sample cell with a spot size of 1 mm diameter where it was merged with the white probe pulse in a close angle (<10°). The probe beam after passing through the 2 mm sample cell was focused on a fibre optic cable that was connected to a CMOS spectrograph for recording the time-resolved spectra (λ = 410–800 nm). Typically, 1500 excitation pulses were averaged for 3 s to obtain the transient spectrum at a set delay time. Kinetic traces at appropriate wavelengths were assembled from the time-resolved spectral data.

Nanosecond transient absorption spectral measurements were made according to the following procedure. An N_2 or O_2 saturated PhCN solutions containing CNH-sp-NH_3^+ (0.5 mg mL^{-1}) was excited by a Panther OPO pumped Nd:YAG laser (Continuum, SLII-10, 4–6 ns fwhm) at 450 nm. The resulting time-resolved transient absorption spectra were measured by using a continuous Xe-lamp (150 W) and a photodiode (Hamamatsu 2949) as the probe light and detector, respectively. The output from the photodiode and the photomultiplier tube was recorded using a digitizing oscilloscope (Tektronix, TDS3032, 300 MHz). The solutions were deoxygenated by N_2 purging for 10 min prior to measurements. Rates of decay of triplet excited state of CNH-sp-NH_3^+ were determined from the disappearance of the absorption band at 590 nm. First-order rate constants were determined by a least-squares curve fit. All experiments were performed at 298 K.

Acknowledgements

The research at Osaka University was supported by Grant-in-Aid (no. 20108010 to SF and no. 23750014 to KO) and Global COE program, "the Global education and Research Centre for Bio-Environmental Chemistry" from the Ministry of Education, Culture, Sports, Science and Technology, Japan and by WCU (R31-2008-000-10010-0) and GRL (2010-00353) programs of KOSEF/MEST, Korea. The research at University of Castilla-La Mancha was supported by the Ministry of Economy and Competitiveness of Spain (projects CTQ2010–17498/BQU and PLE-2009-0038). We thank to Michiko Irie (AIST) for TEM images.

Notes and references

1 S. Iijima, *Nature*, 1991, **354**, 56–58.
2 R. H. Baughman, A. A. Zakhidov and W. A de Heer, *Science*, 2002, **297**, 787–792.
3 (*a*) D. M. Guldi and N. Martín, *Carbon Nanotubes and Related Structures*, VCH, Weinheim, Germany, 2010; (*b*) V. N. Popov and P. Lambin, *Carbon Nanotubes*, Springer, Dordrecht, 2006; (*c*) *Supramolecular Chemistry of Fullerenes and Carbon Nanotubes*, ed. N. Martín and J.-F. Nierengarten, Wiley-VCH, Weinheim, 2011, ch. pp. 10–12.
4 (*a*) X. Peng and S. S. Wong, *Adv. Mater.*, 2009, **21**, 625–642; (*b*) P. Singh, S. Campidelli, S. Giordani, D. Bonifazi, A. Bianco and M. Prato, *Chem. Soc. Rev.*, 2009, **38**, 2214–2230; (*c*) Y. L. Zhao and J. F. Stoddart, *Acc. Chem. Res.*, 2009, **42**, 1161–1171; (*d*) H. Wang, *Curr. Opin. Colloid Interface Sci.*, 2009, **14**, 364–371; (*e*) D. Eder, *Chem. Rev.*, 2010, **110**, 1348–1385; (*f*) A. Hirsch, *Nat. Mater.*, 2010, **9**, 868–871; (*g*) G. Bottari, O. Trukhina, M. Ince and T. Torres, *Coord. Chem. Rev.*, 2012, **256**, 2453–2477.
5 (*a*) L. Yan, Y. B. Zheng, F. Zhao, S. Li, X. Gao, B. Xu, P. S. Weiss and Y. Zhao, *Chem. Soc. Rev.*, 2012, **41**, 365–375; (*b*) T. M. Swager, *ACS Macro Lett.*, 2012, **1**, 3–5; (*c*) Z. Sun, D. K. James and J. M. Tour, *J. Phys. Chem. Lett.*, 2011, **2**, 2425–2432; (*d*) T. Umeyama and H. Imahori, *J. Phys. Chem. C*, 2013, **117**, 3195–3209; (*e*) Y.-P. Sun, K. Fu, Y. Lin and W. Huang, *Acc. Chem. Res.*, 2002, **35**, 1096–1104.
6 (*a*) D. M. Guldi and R. D. Costa, *J. Phys. Chem. Lett.*, 2013, **4**, 1489–1501; (*b*) F. G. Brunetti, C. Romero-Nieto, J. López-Andarias, C. Atienza, J. L. López, D. M. Guldi and N. Martín, *Angew. Chem., Int. Ed.*, 2013, **52**, 2180–2184.
7 (*a*) C. Romero-Nieto, R. García, M. Á. Herranz, C. Ehli, M. Ruppert, A. Hirsch, D. M. Guldi and N. Martín, *J. Am. Chem. Soc.*, 2012, **134**, 9183–9192; (*b*) M. A. Herranz, C. Ehli, S. Campidelli, M. Gutierrez, G. L. Hug, K. Ohkubo, S. Fukuzumi, M. Prato, N. Martín and D. M. Guldi, *J. Am. Chem. Soc.*, 2008, **130**, 66–73; (*c*) Y. Maeda, J. Higo, Y. Amagai, J. Matsui, K. Ohkubo, Y. Yoshigoe, M. Hashimoto, K. Eguchi, M. Yamada, T. Hasegawa, Y. Sato, J. Zhou, J. Lu, T. Miyashita, S. Fukuzumi, T. Murakami, K. Tohji, S. Nagase and T. Akasaka, *J. Am. Chem. Soc.*, 2013, **135**, 6356–6362.
8 (*a*) T. Hasobe, S. Fukuzumi and P. V. Kamat, *J. Am. Chem. Soc.*, 2005, **127**, 11884–11885; (*b*) T. Hasobe, S. Fukuzumi and P. V. Kamat, *J. Phys. Chem. B*, 2006, **110**, 25477–25484; (*c*) K. Saito, H. Qiu, V. Troiani, N. Solladié, T. Sakata, H. Mori, M. Ohama and S. Fukuzumi, *J. Phys. Chem. C*, 2007, **111**, 1194–1199.
9 (*a*) V. Sgobba and D. M. Guldi, *Chem. Soc. Rev.*, 2009, **38**, 165–184; (*b*) C. Gao, Z. Guo, J.-H. Liu and X.-J. Huang, *Nanoscale*, 2012, **4**, 1948–1963; (*c*) S. Cataldo, P. Salice, E. Menna and B. Pignataro, *Energy Environ. Sci.*, 2012, **5**, 5919–5940.
10 (*a*) S. Iijima, M. Yudasaka, R. Yamada, S. Bandow, K. Suenaga, F. Kokai and K. Takahashi, *Chem. Phys. Lett.*, 1999, **309**, 165–170; (*b*) M. Vizuete, M. J. Gómez-Escalonilla, J. L. G. Fierro, M. Yudasaka, S. Iijima,

M. Vartanian, J. Iehl, J.-F. Nierengarten and F. Langa, *Chem. Commun.*, 2011, **47**, 12771–12773.

11 (*a*) N. Karousis, Y. Sato, K. Suenaga and N. Tagmatarchis, *Carbon*, 2012, **50**, 3909–3914; (*b*) N. Karousis, T. Ichihashi, M. Yudasaka, S. Iijima and N. Tagmatarchis, *Chem. Commun.*, 2011, **47**, 1604–1606.

12 (*a*) A. S. D. Sandanayaka, O. Ito, T. Tanaka, H. Isobe, E. Nakamura, M. Yudasaka and S. Iijima, *New J. Chem.*, 2009, **33**, 2261–2266; (*b*) S. Zhu and G. Xu, *Nanoscale*, 2010, **2**, 2538–2549.

13 L. Dai, *Acc. Chem. Res.*, 2013, **46**, 31–42.

14 M. S. Dresselhaus, G. Dresselhaus and P. C. Eklund, *Science of Fullerenes and Carbon Nanotubes*, Academic Press, San Diego, CA, 1996.

15 (*a*) S. Campidelli, M. Meneghetti and M. Prato, *Small*, 2007, **3**, 1672–1676; (*b*) F. Lan and G. Li, *Nano Lett.*, 2013, **13**, 2086–2091; (*c*) N. M. Dissanaake and Z. Zhong, *Nano Lett.*, 2011, **11**, 286–290.

16 K. Urita, S. Seki, S. Utsumi, D. Noguchi, H. Kanoh, H. Tanaka, Y. Hattori, Y. Ochiai, N. Aoki, M. Yudasaka, S. Iijima and K. Kaneko, *Nano Lett.*, 2006, **6**, 1325–1328.

17 (*a*) N. Karousis, N. Tagmatarchis and D. Tasis, *Chem. Rev.*, 2010, **110**, 5366–5397; (*b*) F. D'Souza and O. Ito, *Chem. Soc. Rev.*, 2012, **41**, 86–96.

18 (*a*) F. Rueda, D. M. Guldi and T. Torres, *J. Am. Chem. Soc.*, 2007, **129**, 5061–5068; (*b*) S. Campidelli, C. Sooambar, E. L. Diez, C. Ehli, D. M. Guldi and M. Prato, *J. Am. Chem. Soc.*, 2006, **128**, 12544–12552; (*c*) C. Ehli, G. M. A. Rahman, N. Jux, D. Balbinot, D. M. Guldi, F. Paolucci, M. Marcaccio, D. Paolucci, M. Melle-Franco, F. Zerbetto, S. Campidelli and M. Prato, *J. Am. Chem. Soc.*, 2006, **128**, 11222–11231; (*d*) M. Á. Herranz, N. Martín, S. Campidelli, M. Prato, G. Brehm and D. M. Guldi, *Angew. Chem., Int. Ed.*, 2006, **45**, 4478–4482; (*e*) M. Á. Herranz, C. Ehli, S. Campidelli, M. Gutierrez, G. L. Hug, K. Ohkubo, S. Fukuzumi, M. Prato, N. Martín and D. M. Guldi, *J. Am. Chem. Soc.*, 2008, **130**, 66–73; (*f*) M. Álvaro, P. Atienzar, P. de la Cruz, J. L. Delgado, V. Troiani, H. García, F. Langa, A. Palkar and L. Echegoyen, *J. Am. Chem. Soc.*, 2006, **128**, 6626–6635; (*g*) C. Oelsner, M. A. Herranz, C. Ehli, M. Prato and D. M. Guldi, *J. Am. Chem. Soc.*, 2011, **133**, 18696–18706.

19 (*a*) M. Álvaro, C. Aprile, B. Ferrer and H. García, *J. Am. Chem. Soc.*, 2007, **129**, 5647–5655; (*b*) C. Aprile, R. Martín, M. Alvaro, H. García and J. C. Scaiano, *Chem. Mater.*, 2009, **21**, 884–890; (*c*) R. Martín, F. J. Céspedes-Guirao, M. de Miguel, F. Fernández-Lázaro, H. García and Á. Sastre-Santos, *Chem. Sci.*, 2012, **3**, 470–475.

20 (*a*) C. Ehli, C. Oelsner, D. M. Guldi, A. Mateo-Alonso, M. Prato, C. Schmidt, C. Backes, F. Hauke and A. Hirsch, *Nat. Chem.*, 2009, **1**, 243–249; (*b*) R. Yuge, M. Yudasaka, S. Maigné, M. Tomonari, J. Miyawaki, J. Kubo, H. Imai, T. Ichihashi and S. Iijima, *J. Phys. Chem. C*, 2008, **112**, 5416–5422.

21 (*a*) M. Vizuete, M. Barrejón, M. J. Gómez-Escalonilla and F. Langa, *Nanoscale*, 2012, **4**, 4370–4381; (*b*) A. S. D. Sandayanaka, E. Maligaspe, T. Hasobe, O. Ito and F. D'Souza, *Chem. Commun.*, 2010, **46**, 8749–8751; (*c*) F. D'Souza, R. Chitta, A. S. D. Sandanayaka, N. K. Subbaiyan, L. D'Souza, Y. Araki and O. Ito, *J. Am. Chem. Soc.*, 2007, **129**, 15865–15871; (*d*) F. D'Souza, E. Maligaspe, K. Ohkubo, M. E. Zandler, N. K. Subbaiyan and S. Fukuzumi, *J. Am. Chem. Soc.*, 2009, **131**, 8787–8797.

22 (*a*) S. Fukuzumi and K. Ohkubo, *J. Mater. Chem.*, 2012, **22**, 4575–4587; (*b*) S. Fukuzumi, K. Saito, K. Ohkubo, T. Khoury, Y. Kashiwagi, M. A. Absalom, S. Gadde, F. D'Souza, Y. Araki, O. Ito and M. J. Crossley, *Chem. Commun.*, 2011, **47**, 7980–7982.

23 (*a*) G. Pagona, A. S. D. Sandanayaka, A. Maigne, J. Fan, G. C. Papavassiliou, I. D. Petsalakis, B. R. Steele, M. Yudasaka, S. Iijima, N. Tagmatarchis and O. Ito, *Chem.–Eur. J.*, 2007, **13**, 7600–7607; (*b*) G. Rotas, A. S. D. Sandanayaka, N. Tagmatarchis, T. Ichihashi, M. Yudasaka, S. Iijima and O. Ito, *J. Am. Chem. Soc.*, 2008, **130**, 4725–4731; (*c*) A. S. D. Sandanayaka, O. Ito, M. Zhang, K. Ajima, S. Iijima, M. Yudasaka, T. Murakami and K. Tsuchita, *Adv. Mater.*, 2009, **21**, 4366–4371; (*d*) M. Vizuete, M. J. Gómez-Escalonilla, J. L. G. Fierro, A. S. D. Sandanayaka, T. Hasobe, M. Yudasaka, S. Iijima, O. Ito and F. Langa, *Chem.–Eur. J.*, 2010, **16**, 10752–10763.

24 F. Ajamaa, T. M. F. Duarte, C. Bourgogne, M. Holler, P. W. Fowler and J.-F. Nierengarten, *Eur. J. Org. Chem.*, 2005, 3766–3774.

25 Y. Araki, R. Chitta, A. S. D. Sandanayaka, K. Langenwalter, S. Gadde, M. E. Zandler, O. Ito and F. D'Souza, *J. Phys. Chem. C*, 2008, **112**, 2222–2229.

26 K. Pokhodnia, J. Demsar, A. Omerzu, D. Mihailovic and H. Kuzmany, *Synth. Met.*, 1997, **85**, 1749–1750.

27 J. Park, P. Deria and M. J. Therien, *J. Am. Chem. Soc.*, 2011, **133**, 17156–17159.

28 B. F. Habenicht and O. V. Prezhdo, *J. Am. Chem. Soc.*, 2012, **134**, 15648–15651.

29 (*a*) J. W. Arbogast, A. P. Darmanyan, C. S. Foote, Y. Rubin, F. N. Diederich, M. M. Álvarez, S. J. Anz and R. L. Whetten, *J. Phys. Chem.*, 1991, **95**, 11–12; (*b*) S. Fukuzumi, H. Imahori, H. Yamada, M. E. El-Khouly, M. Fujitsuka, O. Ito and D. M. Guldi, *J. Am. Chem. Soc.*, 2001, **123**, 2571–2575.

30 (*a*) S. Fukuzumi, K. Ohkubo, H. Imahori, J. Shao, Z. Ou, G. Zheng, Y. Chen, R. K. Pandey, M. Fujitsuka, O. Ito and K. M. Kadish, *J. Am. Chem. Soc.*, 2001, **123**, 10676–10683; (*b*) K. Ohkubo, J. Shao, Z. Ou, K. M. Kadish, G. Li, R. K. Pandey, M. Fujitsuka, O. Ito, H. Imahori and S. Fukuzumi, *Angew. Chem., Int. Ed.*, 2004, **43**, 853–856.

31 Y. Kawashima, K. Ohkubo and S. Fukuzumi, *J. Phys. Chem. A*, 2012, **116**, 8942–8948.

32 Á. Sastre-Santos, C. Parejo-Parados, L. Martín-Gomis, K. Ohkubo, F. Fernández-Lázaro and S. Fukuzumi, *J. Mater. Chem.*, 2011, **21**, 1509–1515.

33 (*a*) H. Imahori, D. M. Guldi, K. Tamaki, Y. Yoshida, C. Luo, Y. Sakata and S. Fukuzumi, *J. Am. Chem. Soc.*, 2001, **123**, 6617–6628; (*b*) H. Imahori, Y. Sekiguchi, Y. Kashiwagi, T. Sato, Y. Araki, O. Ito, H. Yamada and S. Fukuzumi, *Chem.–Eur. J.*, 2004, **10**, 3184–3196; (*c*) D. M. Guldi,

H. Imahori, K. Tamaki, Y. Kashiwagi, H. Yamada, Y. Sakata and S. Fukuzumi, *J. Phys. Chem. A*, 2004, **108**, 541–548.
34 S. Tretiak, *Nano Lett.*, 2007, **7**, 2201–2206.
35 W. L. F. Armarego and D. D. Perrin, *Purification of Laboratory Chemicals*, Pergamon Press, Oxford, 1997.
36 M. Zhang, M. Yudasaka, K. Ajima, J. Miyawaki and S. Iijima, *ACS Nano*, 2007, **1**, 265.